

Period doubling, two-color lattices, and the growth of swallowtails in Bose-Einstein condensates

B. T. Seaman, L. D. Carr, and M. J. Holland

*JILA, National Institute of Standards and Technology and Department of Physics,
University of Colorado, Boulder, CO 80309-0440*

(Dated: January 23, 2018)

The band structure of a Bose-Einstein condensate is studied for lattice traps of sinusoidal, Jacobi elliptic, and Kronig-Penney form. It is demonstrated that the physical properties of the system are independent of the choice of lattice. The Kronig-Penney potential, which admits a full exact solution in closed analytical form, is then used to understand in a novel way the swallowtails, or loops, that form in the band structure. Their appearance can be explained by adiabatically tuning a second lattice with half the period. Such a two-color lattice, which can be easily realized in experiments, has intriguing new physical properties. For instance, swallowtails appear even for weak nonlinearity, which is the experimental regime. We determine the stability properties of this system and relate them to current experiments.

PACS numbers: 03.75.Hh, 03.75.Lm, 03.65.Ge

I. INTRODUCTION

There has been great interest in the study of Bose-Einstein condensates (BEC's) from both the experimental and theoretical perspective since they were first created in 1995 [1, 2, 3]. In particular, the examination of BEC's in periodic potentials in the superfluid phase has yielded many intriguing phenomena, such as gap solitons [4, 5], the appearance of swallowtails or loops in the band structure, pulsed atom lasers and demonstrations of their phase coherence [6, 7], and matter-wave diffraction [8]. BEC's in periodic potentials, unlike other solid state systems, have the advantage that the lattice geometry and interatomic interactions are highly controllable [9, 10]. We examine the mean field Bloch states of a BEC in a one-color and two-color potential for arbitrary interaction and potential strengths. The full nonlinear band structure of the system is then determined for a two-color potential. We show that period-doubled states in the usual one-color lattice are directly connected with Bloch waves in the two-color case. Period-doubled states have a periodicity which is twice that of the underlying lattice. This allows for a novel interpretation of swallowtails, a key physical property of the band structure of a BEC. The study of period-doubled states has been important in other systems, for instance in optics [11, 12], because it offers experimental access to the period-doubling route to chaos.

The band structure of a BEC in an optical lattice has previously been studied both analytically and numerically. An array of techniques have been developed. The sinusoidal potential, which is the experimental case, has been investigated by expanding the wavefunction in a Fourier series and minimizing the energy [13, 14, 15, 16, 17]. Two other potentials have been studied in detail. A Jacobi elliptic potential, which asymptotically approaches the sinusoidal case, has the advantage that it emits a useful class of exact solutions [18, 19, 20]. On the other hand, the Kronig-Penney

potential can be solved completely and exactly, as we have shown in our previous work [21, 22, 23]. We compare these three models with the aid of the Bloch wave representation. For the Jacobi elliptic potential this requires a reinterpretation of the original result [18]. In addition, we explain the longstanding open problem of why certain density offsets in this class of solutions lead to instability. We find that the form of the potential has no effect on the superfluid and other physical properties of the system. Of the closed-form analytical methods available for the three potentials, only the Kronig-Penney potential admits a full description of the band structure.

The two-color lattice has already received some attention in the literature. Roth and Burnett showed that when the period of the second lattice is much longer than the first, so that it forms an envelope, new quantum phases are introduced into the quantum problem [24]. We will consider the superfluid phase only, which is obtained when the lattice height is on the order of or smaller than the chemical potential. Very recently, Louis *et al.* have studied gap solitons in a two-color lattice for which the second lattice has half the period of the first [25]. We study the same potential, but for Bloch waves, rather than gap solitons. Bloch waves have the same period as the lattice, whereas gap solitons are envelope solutions. Using the Kronig-Penney potential, we link the period-doubled states of the one-color lattice to Bloch waves in the two-color case. Adiabatically turning off one of the frequencies in a two-color lattice, one can clearly observe the origin of swallowtails. Unlike previous explanations of this intriguing property of nonlinear periodic systems [26], ours encompasses both repulsive and attractive BEC's.

Experiments on BEC's in optical lattice potentials proceed as follows. Alkali-metal bosonic atoms are cooled to the quantum degenerate regime. The interference pattern of two counter propagating lasers is used to create a sinusoidal potential shift caused by the ac Stark effect induced by the dipole interaction with the laser

field on the atoms' center of mass motion [27, 28]. A small frequency detuning of one of the lasers allows for examination of the different quasimomentum states and their stability properties by creating a traveling wave interference pattern moving at the velocity $v = (\lambda/2)\delta\nu$, where λ is the wavelength of the first beam and $\delta\nu$ is the detuning [29, 30, 31]. The two-color lattice can then be created by the superposition of two lasers with frequencies which differ by a factor of two. This can be achieved using second harmonic generation with nonlinear crystals. Complex lattice configurations with several lasers have already been performed experimentally [32]. We present a dynamical study of key observables for the two-color lattice, such as the instability time, that can be experimentally investigated with minor changes to current apparatus. There have been many theoretical studies of stability properties of BEC's in one-color lattices (see [18, 19, 20, 33, 34, 35, 36], to name a few), though not of the two-color case. We take advantage of the analytical simplicity of the Kronig-Penney potential in order to correctly seed our numerical studies of the mean field.

Thus, the three main objectives of this article are the following. First, in Secs. II and III, the qualitative properties of a condensate in a periodic potential are shown to be independent of the specific form of the potential. This justifies the use of a Kronig-Penney potential for the rest of our study. Second, in Sec. IV, the nonlinear band structure of the two-color lattice is described fully and analytically. This is used to interpret the appearance of swallowtails in the one-color lattice in a novel way. Third, in Sec. V, numerical simulations are used to make a connection between the properties of the two-color lattice and current experiments on BEC's in one-color lattices. Finally, concluding remarks are made in Sec. VI.

II. THE NONLINEAR SCHRÖDINGER EQUATION AND BLOCH WAVES

The stationary states of the mean field of a BEC in an external periodic potential $V(x)$ are governed by the nonlinear Schrödinger equation [37, 38, 39], also called the Gross-Pitaevskii equation [40, 41],

$$-\frac{1}{2}\Psi_{xx} + g|\Psi|^2\Psi + V(x)\Psi = \mu\Psi, \quad (1)$$

where μ is the eigenvalue and g characterizes the effective quasi-one-dimensional two-body atomic interaction. A quasi-one dimensional condensate can be created by making an elongated trap that is tightly bound in the transverse directions. In Eq. (1), length has been scaled by the lattice spacing d and energy has been scaled by $2E_0/\pi^2$ where

$$E_0 \equiv \frac{\hbar^2\pi^2}{2md^2} \quad (2)$$

is the recoil energy, or kinetic energy of a particle at the edge of the first Brillouin zone, and m is the particle's

mass. With this scaling, the renormalized 1D coupling is $g \equiv 2a_s\omega md/\hbar$, where harmonic confinement in the transverse directions has been assumed with frequency ω , and a_s is the two body s -wave scattering length.

The wavefunction Ψ is given by

$$\Psi = \sqrt{\rho(x)} \exp[i\phi(x) - i\mu t], \quad (3)$$

where $\rho(x)$ is the linear density of the condensate and the local superfluid velocity is given by $v = \partial\phi/\partial x$. Substituting Eq. (3) into Eq. (1), one finds that the phase is related to the density by

$$\phi(x) = \alpha \int_0^x \frac{dx'}{\rho(x')}, \quad (4)$$

where α is a real constant of integration. Note that we have chosen $\phi(0) = 0$.

When describing the band structure of a system, one constructs the solutions in the usual Bloch form,

$$\Psi(x) = e^{iqx} f_q(x), \quad (5)$$

where q is the quasimomentum and $f_q(x) = f_q(x+1)$, i.e., has the same period as the lattice. The band structure $E(q)$ can be determined from the relationship between the quasimomentum and the energy per particle in terms of the density and phase of the solution:

$$q = \alpha \int_0^1 \frac{dx'}{\rho(x')}, \quad (6)$$

$$\frac{E}{n} = \frac{1}{n} \int_0^1 dx' \left(\frac{1}{2} |\partial_{x'} \Psi|^2 + \frac{g}{2} |\Psi|^4 + V(x') |\Psi|^2 \right), \quad (7)$$

where E/n is the energy per atom, q is the quasimomentum, and n is the number of atoms per lattice site. The latter is given by the normalization

$$n = \int_0^1 dx' \rho(x'). \quad (8)$$

The quasimomentum is the phase jump between adjacent sites of the lattice and is proportional to the mean superfluid velocity of the system. We scale the quasimomentum by

$$q_0 \equiv \pi/d, \quad (9)$$

which is the quasimomentum at the edge of the Brillouin zone.

The band structure is modified from the well-known solutions of the linear Schrödinger equation with a periodic potential. There are two physical regimes [21]. For $|g|n \leq V_0$, which we term the regime of *weak nonlinearity*, the linear band structure is simply perturbed up or down, depending on the sign of g . For $|g|n \gg V_0$, which corresponds to the regime of *strong nonlinearity*, the bands wrap back around on themselves to form loop structures, or swallowtails. These swallowtails have previously been described in terms of the superfluid screening properties

of the condensate [26]. This explanation is only valid for repulsive condensates, despite the fact that swallow-tails also appear in the attractive case. This motivates the need for another explanation, which we provide in Sec. IV.

There have been many methods used to determine the nonlinear band structure of BEC's in periodic structures. In the following section, three analytical methods are described and evaluated. In addition to these analytical approaches, many numerical methods have been developed. These include Hamiltonian perturbation theory [42] and the study of accelerating lattices [43]. We consider only analytical methods of obtaining stationary states.

III. ANALYTICAL METHODS IN NONLINEAR BAND THEORY

Of the many methods used in nonlinear band theory, analytical methods allow for greater flexibility in describing solution types, as they result in general expressions which describe all parameter regimes simultaneously. In this section, we compare three methods that use different periodic potentials and interpret their solutions in the Bloch wave representation. It is found that they all produce the same band structure for the lowest band. Hence, the exact form of the potential is unimportant. Nevertheless, only the method based on the Kronig-Penney potential is able to describe all bands analytically since an exact solution method exists for piecewise constant potentials [21, 38, 44].

A. Solution by Cancellation

The first analytical method for obtaining solutions to the NLS with a periodic potential in the context of a BEC was given by Bronski, Carr, Deconinck, and Kutz [18] for a Jacobi elliptic potential of form

$$V(x) = -V_0\{1 - 2\text{sn}^2[2K(k)x, k]\}, \quad (10)$$

where sn is one of the Jacobi elliptic functions [45]. The Jacobi elliptic functions are generalized periodic functions characterized by an elliptic parameter $k \in [0, 1]$. They approach circular and hyperbolic trigonometric functions as $k \rightarrow 0$ and $k \rightarrow 1$, respectively. For k not exponentially close to unity, the potential is similar to the sinusoidal case. As k approaches unity, the period of the lattice becomes much greater than the width of the localized variations of the potential, thereby approaching a lattice of delta functions, i.e., a Kronig-Penney potential. The period of the lattice is $2K(k) \in [\pi, \infty]$ where $K(k)$ is a complete elliptic integral of the first kind [45].

Bronski *et al.* were able to show that it is possible to choose a suitable ansatz for the density such that the nonlinear term cancels the potential term, thereby leaving a system that is effectively free. They found a special

class of solutions with a period equal to that of the lattice, where the density was assumed to be of the form

$$\rho(x) = A\text{sn}^2(bx, k) + B. \quad (11)$$

The following conditions must then be met:

$$A = \frac{b^2k^2 + 2V_0}{g}, \quad (12)$$

$$\alpha^2 = B(B + A)(b^2 + Bg - \frac{2BV_0}{A}), \quad (13)$$

$$\mu = \frac{1}{2}(b^2 + Ag + 3Bg) - \frac{BV_0}{A}. \quad (14)$$

Machholm *et al.* [16] showed that this solution corresponds to the edge of the Brillouin zone for the exactly sinusoidal case, $k = 0$. If the parameters of the potential, V_0 , k , and b , and the interaction strength gn are set, the wavefunction is completely determined without any free parameters. Nevertheless, the solutions are of more general use. In fact, although not described in this way by the original authors, this family of solutions can be used to map out the whole lowest energy band. It is possible to change the elliptic parameter k to get a spectrum of solutions. Since the Jacobi elliptic functions closely approximate the trigonometric functions for all k except exponentially close to unity, there is a wide range of values for k where the potential is approximately sinusoidal. In addition, the sign of the potential coefficient V_0 does not significantly change the form of the potential and so this is another parameter that can be changed to determine the energy bands. Therefore, when the elliptic parameter is varied, and the solutions determined via Eqs. (11)-(14), the complete lowest energy band can be analytically determined for arbitrary interaction strength.

An example of the band structure for strong nonlinearity is shown in Fig. 1(a). The interaction strength is chosen to be a factor of ten larger than the strength of the potential, causing the appearance of swallowtails. Only the lowest energy band can be extracted with this class of solutions. This shows that these simple exact solutions are sufficient to describe measurable properties of the condensate such as breakdown of superfluidity for critical values of the nonlinearity [26, 31].

In the work of Bronski *et al.* [18, 19], the linear stability properties of the solutions were proved for the case of constant, or trivial phase. No such proof was discovered for the case of non-trivial phase solutions. The latter are, for example, the only stable ones in the exactly sinusoidal case of $k = 0$. It was found numerically that non-trivial phase solutions for repulsive condensates with large offsets B were stable, while for smaller B they were unstable. No explanation for this stability property was found. After we recast the solutions in Bloch form and used them to determine the band structure, the stability properties become immediately apparent. Solutions on the upper edge of the swallowtail are known to be unstable, as they represent an energy maximum [16, 21, 26]; these correspond to small B . Solutions on the main part of the

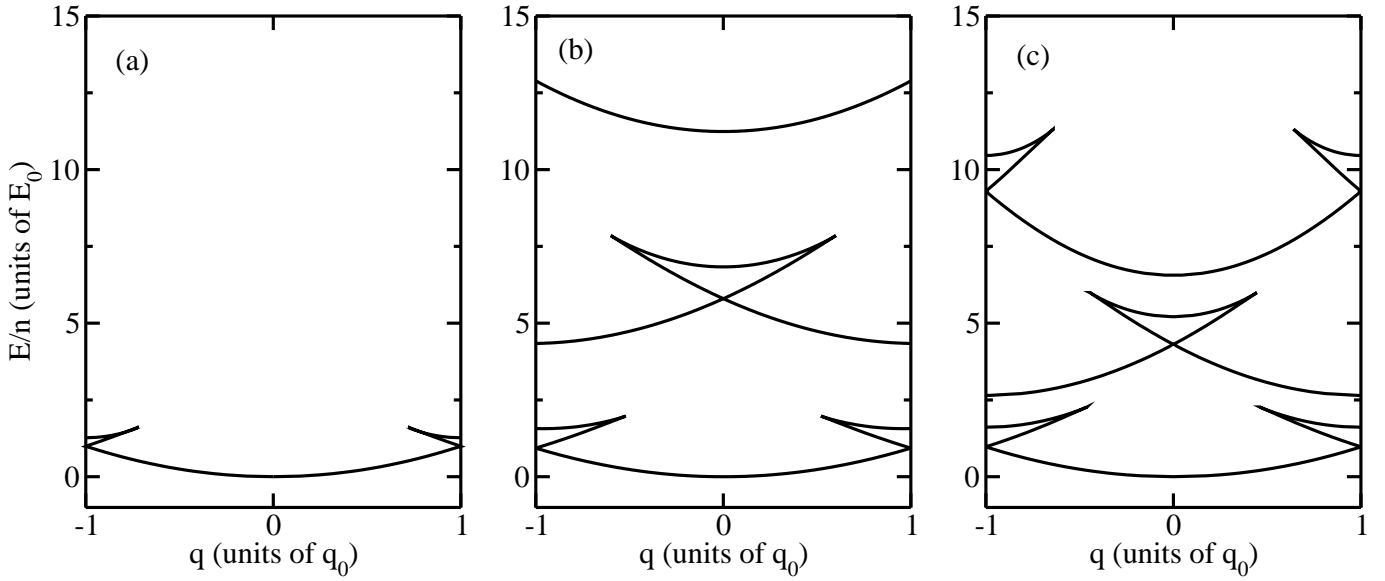


FIG. 1: Band structure for a strongly repulsive condensate, $gn = 10$, in a periodic potential. Shown are results obtained via the analytical methods of (a) Bronski *et al.* [18] with a Jacobi elliptic potential ($|V_0| = 1$), (b) Machholm *et al.* [16] with a sinusoidal potential ($V_0 = 4$), and (c) Seaman *et al.* [21] with a Kronig-Penney potential ($V_0 = 1$).

band and the lower edge of the swallowtail represent an energy minimum and are stable; these correspond to large B . For instance, in Fig. 1(a), the main part of the band from $q = 0$ to $q = 1$ corresponds to $B \in [0.559, 0.509]$; the lower edge of the swallowtail near the edge of the Brillouin zone corresponds to $B \in [0.509, 0.277]$; and the upper edge, which is unstable, corresponds to $B \in [0.277, 0]$. We note that, in comparing with Bronski *et al.*, they normalized the wavefunction to gn rather than having gn as the coefficient of the nonlinearity in the NLS. In their numerical studies of stability, they did not hold their normalization (our nonlinear coefficient) fixed. In Fig. 1(a), we fix the nonlinearity to be $gn = 10|V_0|$.

B. Solution by Three Mode Approximation

In a subsequent work by Machholm, Pethick and Smith [16], a more complete method to determine the nonlinear band structure was introduced that used a sinusoidal potential

$$V(x) = 2V_0 \cos^2(\pi x). \quad (15)$$

The wavefunction was expanded in a Fourier series for a particular quasimomentum and the energy was minimized. This method uses the exact physical form of the typical experimental lattice potential that a BEC is held in but requires the root finding of many free parameters. Machholm *et al.* showed that one can obtain analytical solutions by using a three-mode Fourier spectrum:

$$\Psi(x) = \sqrt{n} e^{iqx} (a_0 + a_1 e^{i2\pi x} + a_{-1} e^{-i2\pi x}), \quad (16)$$

where a_0 , a_1 and a_{-1} are real coefficients. Due to the normalization condition on the wavefunction, there are two real free parameters of the solution.

Using the three-mode expansion of the wavefunction, it is possible to extract the first two bands and the lower part of the third band, as shown in Fig. 1(b). Notice that, unlike with the previous method, full information from the first two bands can be extracted, instead of only the lowest band. However, the three-mode approximation overestimates the width of the swallowtails [16]. If more Fourier components are included, for a total between five and ten, the first three bands can be described to within 1% accuracy. For higher bands even more Fourier components are needed. This method was later extended to include period-doubled states [17].

In addition to determining the band structure, Machholm *et al.* were able to determine several analytical expressions associated with the stability properties of the condensate. In particular, the interaction strength at which swallowtails first appear in the lowest band, and the width of the swallowtails for a given interaction strength were determined analytically. Studies of the stability of the condensate to small perturbations were also performed.

C. Solution via a Piece-wise Constant Lattice

In comparison, in our previous work [21] a lattice of delta functions, a Kronig-Penney potential, was used

$$V(x) = V_0 \sum_{j=-\infty}^{+\infty} \delta(x - j). \quad (17)$$

We presented the complete set of Bloch waves solutions in analytical form by solving the piece-wise-constant potential case and using the appropriate boundary conditions to fix the parameters of the solution. The potential, however, is quite different from the experimentally created sinusoidal lattice. The optical lattice potential is composed of a single Fourier component while the Kronig-Penney potential is a comb of equally weighted Fourier components. We proved that the most general form of the density over a finite interval of constant potential is given by

$$\rho(x) = B + \frac{k^2 b^2}{g} \text{sn}^2(bx + x_0, k), \quad (18)$$

where again sn is one of the Jacobi elliptic functions. It should be noted that the square of any Jacobi elliptic function can be related linearly with the square of every other Jacobi elliptic function. Thus all twelve Jacobi elliptic functions are possible solutions. The chemical potential μ and phase prefactor α (see Eq. (4)) are given by

$$\begin{aligned} \mu &= \frac{1}{2}[b^2(1 + k^2) + 3Bg], \quad (19) \\ \alpha^2 &= B(k^2 b^2/g + B)(b^2 + Bg). \quad (20) \end{aligned}$$

The energy bands can be determined by varying one of the parameters in the wavefunction, such as B or b , and determining the quasimomentum and the energy from Eqs. (6) and (7). In particular, the parameter scaling b was varied since it is closely related to the quasimomentum. The offset B and elliptic parameter k are determined by number conservation and the boundary conditions across the delta functions.

The first three bands for the Kronig-Penney lattice are presented in Fig. 1(c). Although only the first three bands are presented, our method can be used to determine the higher bands with no additional computational intensity, unlike with the technique of Sec. III B. For all energy bands, all that is required computationally is the root finding of two parameters, the offset B and the elliptic parameter k . The stability properties of the condensate were then numerically determined by dynamically evolving an initial state composed of the stationary solution plus a small amount of white noise. It was found that the stability of the energy bands depends on the interaction strength. For weak nonlinearity, the bands become unstable for quasimomentum greater than approximately $\pi/2$. For strong nonlinearity, the tops of the swallowtails are unstable but the remainder of the first band is stable. The second and higher bands are always unstable.

In spite of the differences in the potentials, all three methods find a similar nonlinear band structure. In addition, the stability properties of the three models were also the same. Therefore, to study the main physical aspects of this system, any method can be used. All three methods are useful in determining the first band. For the

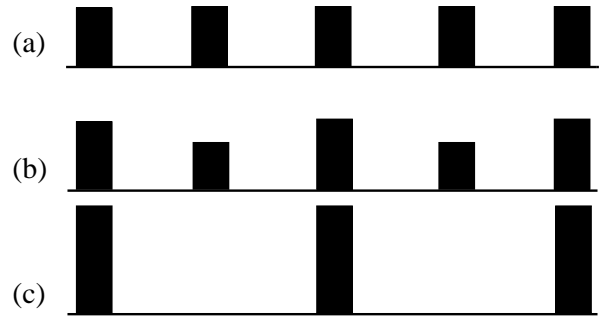


FIG. 2: A sketch of the potential is illustrated for the three cases of Figs. 3 and 4, with appropriately normalized boxes representing delta functions: (a) a one-color lattice of period d and $\Delta = 0$; (b) a two-color lattice with a small difference in the potential strengths, period $2d$ and $\Delta = 0.2$; (c) a one-color lattice with period $2d$ and $\Delta = 1$. Adiabatically tuning the system from (a) to (c) allows for a novel explanation of the appearance of swallowtails in the band structure.

full band structure, only our method is analytically and numerically tractable.

IV. THE TWO-COLOR LATTICE AND FORMATION OF SWALLOWTAILS

Current experiments with BEC's utilize only one-color lattices in the weakly nonlinear regime. Therefore there has been no experimental observation of the swallowtail structure, which requires strong nonlinearity. Two-color lattices, on the other hand, allow one to produce swallowtails even for weak nonlinearity, as we shall show in the following. Moreover, adiabatically tuning the two-color lattice allows for an explanation of swallowtails for both repulsive and attractive BEC's.

A two-color lattice is produced by adding a second frequency component of twice the fundamental frequency, or half the period. Such a straightforward modification of existing experiments can be made via second harmonic generation with nonlinear crystals. In Sec. III we showed that the exact form of the potential is unimportant. Therefore, to study the two-color lattice, we use a Kronig-Penney-like potential with delta functions of two different strengths:

$$V(x) = V_0 \sum_{j=-\infty}^{+\infty} [(1 - \Delta)\delta(x - 2j) + (1 + \Delta)\delta(x - 2j + 1)], \quad (21)$$

where $\Delta \in [0, 1]$. The strengths of the two sublattices are $(1 - \Delta)V_0$ and $(1 + \Delta)V_0$, respectively. The form of Eq. (21) allows the potential to be tuned continuously from the one-color lattice of strength V_0 and period d ($\Delta = 0$) to the one-color lattice of strength $2V_0$ and period $2d$ ($\Delta = 1$). This holds the average potential strength constant. For $0 < \Delta < 1$ the potential is two-color. Figure 2 sketches the progression between the

two lattices, where the delta functions are represented by square functions of fixed width and varying heights. We will show how period-doubled solutions of the $\Delta = 0$ lattice map onto Bloch-wave solutions of the $\Delta = 1$ lattice, including the swallowtails.

The stationary states of the NLS with the potential of Eq. (21) are determined in the same manner as was described in Sec. III C, with the addition of a second boundary condition. Period-doubled solutions can be obtained via the transformation $\Psi(x) = f_q(x) \exp(i2qx)$, while Bloch solutions were found via $\Psi(x) = f_q(x) \exp(iqx)$. In general, one can obtain solutions of the form $\Psi(x) = f_q(x) \exp(imqx)$, with m an integer; we focus on the period-doubled case, $m = 2$, and the Bloch wave case, $m = 1$.

We first illustrate period-doubled solutions for the lattice of Fig. 5(a), $\Delta = 0$. There are two types of period-doubled solutions, *trivial* and *non-trivial*. The trivial period-doubled solutions simply reproduce the Bloch waves. That is to say, solutions of period d are also trivially solutions of period $2d$. These are illustrated in Fig. 3(a) as thin curves for the case of weak nonlinearity. Period-doubled solutions extend across a Brillouin zone of half the quasimomentum-domain as that of Bloch waves. Thus the domain of Fig. 3 ($q \in [0, 1]$) is half that of Fig. 1 ($q \in [-1, 1]$). The bands are required to be symmetric around the center of the Brillouin zone. One reflects the band in the right half of the Bloch Brillouin zone around its center at $q = 0.5$ to obtain the trivial period-doubled solutions. This leads to the two branches which make the form of an ‘x’ in Fig. 3(a) (thin black curves). The non-trivial period-doubled solutions are shown as a thick blue curve in Fig. 3(a). These form a saddle between the trivial solution branches. The form of the density for the non-trivial period-doubled solutions is shown as the solid curve in Fig. 5. The non-trivial solutions are caused by the nonlinearity in Eq. (1); they have no analog in the linear Schrödinger equation. Comparing Fig. 3 to the swallowtails illustrated in Fig. 1, we make the following conjecture: non-trivial period-doubled solutions for a lattice of period d appear as the saddle of the swallowtail for Bloch waves for a lattice of period $2d$.

This conjecture is supported by tuning Δ from zero to unity. We illustrate this tuning in the subsequent panels of Fig. 3. Figure 3(b) shows the case $\Delta \ll 1$. Figure 3(c) shows the endpoint, $\Delta = 1$. The shape of the lattice in the panels (a)-(c) is sketched in Fig. 2. In Fig. 3(b), the trivial and non-trivial period-doubled solutions of Fig. 3(a) separate into two bands. The lower band (solid curve) consists of the lower part of the trivial period-doubled solutions, with the non-trivial period-doubled solutions forming the upper edge of the swallowtail. The upper band (dashed curve) consists of the upper part of the trivial period-doubled solutions. One observes that there is a small gap between the two bands. Moreover, unlike in the case of the one-color lattice, one obtains a swallowtail even for weak nonlinearity. As Δ is increased, this gap increases. Figure 3(c) shows the

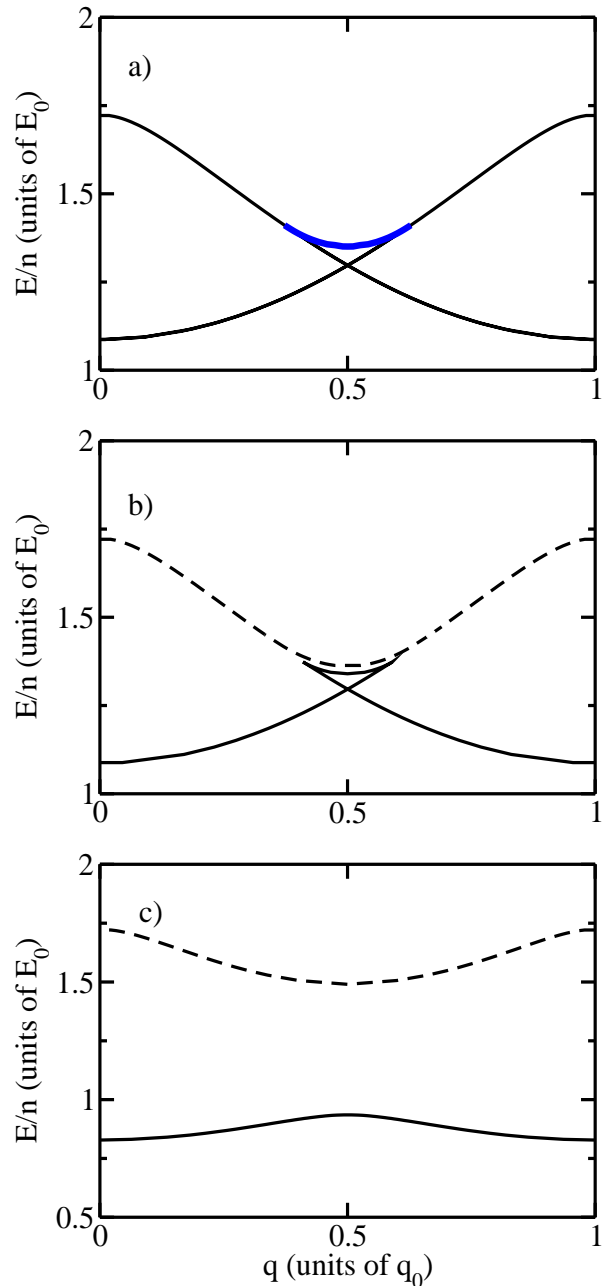


FIG. 3: (color online) Band structure for a two-color lattice with weak nonlinearity, $gn = V_0$. (a) Shown are period-doubled solutions for a one-color lattice of period d and $\Delta = 0$ (Thin black curve: trivial solutions; thick blue curve: non-trivial); (b),(c) Bloch-wave solutions with period $2d$ (Solid curve: lowest band; dashed curve: second band). (b) A two-color lattice with $\Delta \ll 1$. Note that the central swallowtail is derived from the non-trivial period-doubled solution of panel (a). (c) A one-color lattice with $\Delta = 1$. The swallowtail has disappeared due to the weak nonlinearity. The lattices associated with (a)-(c) are sketched in Fig. 2.

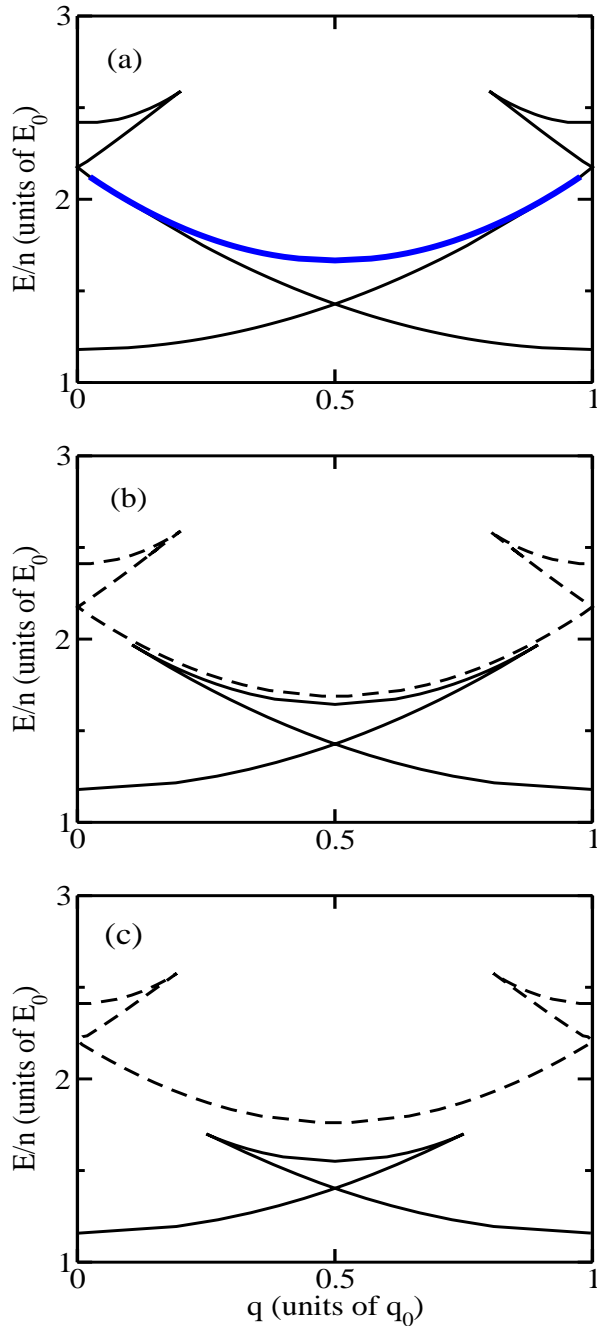


FIG. 4: (color online) Same as Fig. 3 but for strong nonlinearity, $gn = 10V_0$. In (b), (c) note that the upper edge of the central swallowtail in the lower band is derived from the non-trivial period-doubled solution of panel (a) (blue thick curve). The lattices associated with (a)-(c) are sketched in Fig. 2.

case $\Delta = 1$. The system is now again in a weakly nonlinear regime with a one-color lattice. Thus the swallowtail disappears.

One observes that, in general, the first two Bloch-wave bands of a one-color lattice of period $2d$ (panel (c)) can be derived from the trivial period-doubled solutions of a lattice of period d (panel (a)) via a two-color intermediate

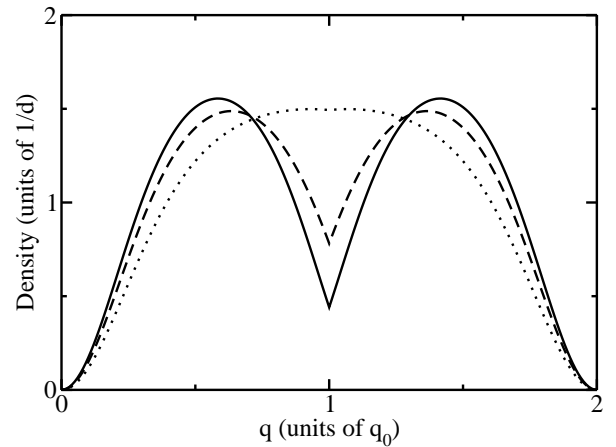


FIG. 5: The condensate density profiles are illustrated for three cases: $\Delta = 0$, non-trivial period-doubled solutions (solid curve); $\Delta = 1/2$, upper edge of the swallowtail (dashed curve); and $\Delta = 1$, the lowest band (dotted curve). The parameters are $q = 0.5$ and $gn = V_0$, which is the regime of weak nonlinearity, as in Fig. 3.

lattice (panel (b)). This follows from the fact that the second Bloch-wave band has two density peaks per site.

In the strongly nonlinear regime, the swallowtail forms in a similar manner but does not disappear for $\Delta = 1$. We illustrate this sequence in Fig. 4, again for $\Delta = 0$, $\Delta \ll 1$, and $\Delta = 1$. One clearly sees that the upper edge of the swallowtail in the one-color lattice of period $2d$ is derived from the non-trivial period-doubled solutions of the one-color lattice of period d . The lower edge of the swallowtail is derived from the trivial period-doubled solutions.

This introduces a novel perspective on the origin of the swallowtails in the nonlinear band structure. In the figures we illustrated the case of a repulsive condensate, as that is the most common experimentally. The same argument holds for attractive condensates, where the swallowtails form below, rather than above the bands. In particular, in our study of the one-color Kronig-Penney potential [21], we found it intriguing that no swallowtail formed on the lowest band for the attractive case.

Previous interpretations of swallowtails were based on the superfluid screening properties of the condensate [26]. In this argument, the condensate sees the quadratic free particle dispersion up to the sound speed. When written in the form of the Bloch ansatz, these quadratic curves repeat in each Brillouin zone. When the sound speed is such that the maximum quasimomentum of each curve overlaps with the curve from the adjoining Brillouin zone, one obtains swallowtails. This does not apply to attractive condensates, since the swallowtails form on the lower edge of the bands and not at all on the lowest band.

In contrast, our argument based on period-doubling applies to both repulsive and attractive condensates. For attractive nonlinearity, the non-trivial period-doubled

states form a convex saddle on the *lower* edge of the ‘x’ of Fig. 3(a), rather than the upper edge. As Δ is tuned from zero to unity, the upper part of the ‘x’ separates from the lower part, carrying the swallowtail with it. Thus no swallowtail can form on the lowest band.

Thus, we understand swallowtails to be adiabatically connected to period-doubled solutions of a lattice of half the period. They originate in non-trivial period-doubling brought about by the nonlinear term in the NLS.

Finally, since the density is a key observable in experiments on BEC’s, in Fig. 5 density profiles are illustrated for weak nonlinearity and $\Delta = 0, 1/2, 1$. The plot is made for quasimomentum $q = 0.5$ and the energy per particle such that the solution lies at the center of the non-trivial period-doubled solution (thick blue curve) in Fig. 3(a), at the top of the central swallowtails on the lowest band in Fig. 3(b), and on the lower band in Fig. 3(c).

V. STABILITY PROPERTIES AND COMPARISON WITH EXPERIMENTS

Several important experiments have been performed with superfluid BEC’s in optical lattices. In particular, an experiment by Fallani *et al.* [29, 46] studied the loss rate of the BEC as the quasimomentum was varied. This loss rate is expected to be monotonically related to the instability time of the condensate. This observable can be modelled theoretically by adding white noise to an initial stationary state on the lattice in simulations. In this way, we investigate the nonlinear stability properties of Bloch-wave solutions to the two-color lattice. Note that unstable solutions which have lifetimes longer than experimental timescales will appear experimentally stable.

In our simulations, Eq. (1) was dynamically evolved using a variable step fourth-order Runge-Kutta algorithm in time and a pseudospectral method in space. We chose periodic boundary conditions in one dimension, with a sufficient number of sites so that the results were independent of the ring circumference. Two schemes for delta functions on a grid were considered: point defects, and narrow square potentials covering several grid points. For square potentials less than one tenth the lattice period d , differences between the two schemes were negligible. Simulations were performed over time scales on the order of those relevant to the experiments, namely, hundreds of milliseconds. The lattice spacing d is taken to be $1 \mu\text{m}$ and the atomic mass to be that of ^{87}Rb .

The stability of the system is quantified by the variance in the Fourier spectrum,

$$\sigma(t) \equiv \frac{\sum (f(p, t) - f(p, 0))^2}{2 \sum (f(p, 0))^2}, \quad (22)$$

where $f(p, t)$ is the Fourier component of the wavefunction at momentum p and time t . The variance approaches unity when the wavefunction has no component in common with the initial state and zero when then the wavefunction it is identical to the initial state. We define

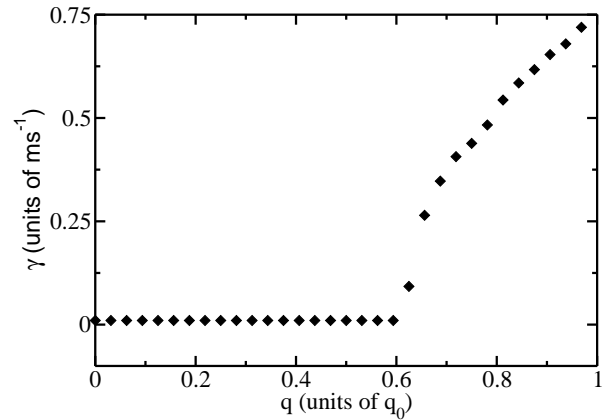


FIG. 6: Shown is the inverse of the instability time $\gamma = T_i^{-1}$ of stationary states in the lowest band, as a function of the quasimomentum. White noise was added to the initial state and the wavefunction was evolved numerically for the NLS with a one-color lattice and weak nonlinearity, $gn = V_0$.

the instability time T_i to occur when the variance has increased to $\sigma = 0.5$.

A clear experimental observable is the rate of loss of atoms from the system, since the density of the sample can be imaged at successive times. This loss rate is expected to be monotonically related to the inverse time in which instabilities arise. Therefore, we present two relevant studies of the instability times of the condensate. First, the growth rate of the instability,

$$\gamma \equiv 1/T_i, \quad (23)$$

is determined for a one-color lattice and weak nonlinearity. This relates directly to the experiment of Fallani *et al.* Second, the lowest positive quasimomentum for which the system becomes unstable is evaluated as a function of Δ for the two-color lattice.

Figure 6 presents the results of the first study. The solutions are stable until the quasimomentum where the nontrivial and trivial period-doubled solutions connect in the band structure (see Fig. 3(a), as well as Ref. [17]). Stability can also be determined from the effective mass of the system,

$$m^* \equiv \frac{1}{\partial^2 E / \partial^2 q}. \quad (24)$$

If the effective mass becomes negative, the NLS becomes effectively attractive. Since the ground state of an attractive condensate is localized, solutions with negative effective mass $m^* < 0$ are unstable. The point where the nontrivial and trivial period-doubled solutions connect corresponds to a change in the sign of the effective mass from positive to negative. Our figure qualitatively replicates the results found by Fallani *et al.* [31] (see figures therein [31]).

Figure 7 presents the second study. In particular, the smallest quasimomentum for which the periodic system

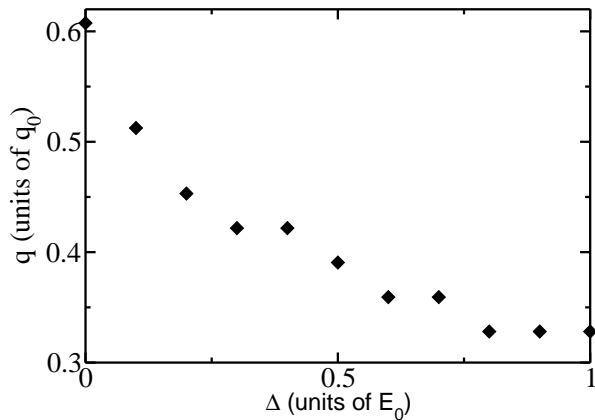


FIG. 7: The lowest positive quasimomentum for which the system becomes unstable is determined as a function of Δ as the one-color lattice of period d is tuned via a two-color lattice to the one-color lattice of period $2d$. The result of simulations of the NLS with weak nonlinearity, $gn = V_0$, are shown.

first becomes unstable in a time less than 100 ms is plotted. The two end points at $\Delta = 0$ and $\Delta = 1$ are easily determined, since those systems are one-color lattices. As per our discussion in the previous paragraph, the Bloch wave solutions become unstable at the point where the non-trivial period-doubled solutions connect to the Bloch-wave band. The two one-color lattice systems have the same ratio of nonlinearity to potential strength, since for $\Delta = 0$ the potential strength is V_0 and the number of atoms is n , while for $\Delta = 1$ they are $2V_0$ and $2n$. Thus the existence of the non-trivial period-doubled states scales with the length of the Brillouin zone. The absolute quasimomentum where instability occurs then differs by a factor of two, since for a lattice of period $2d$ the Brillouin zone is half the length as for d . In Fig. 7, this is $q \sim 0.6$ for $\Delta = 0$ and $q \sim 0.3$ for $\Delta = 1$. In the case of the linear Schrödinger equation, the endpoints would be 0.5 and 0.25, respectively. Note that our simulations are accurate to within a few percent.

The intermediate points in Fig. 7, where $0 < \Delta < 1$ and one obtains a two-color lattice, can be understood by again considering where the effective mass becomes negative. As the energy band from the $\Delta = 0$ lattice separates into the first two bands of the $\Delta = 1$ lattice, the upper edge of the swallowtail shrinks. Recall that states on the lower edge of swallowtails are stable [21]. As Δ is increased, the swallowtail disappears, since the nonlinearity is weak. The quasimomentum at which the band changes from concave up to concave down, i.e. where the effective mass changes sign, moves from right to left, as can be seen in the descending data points of Fig. 7. A

similar argument holds for the case of strong nonlinearity.

VI. CONCLUSION

We have presented a novel way of understanding the appearance of swallowtails in nonlinear band structure. Swallowtails in a lattice of period $2d$ are adiabatically connected to the non-trivial period-doubled solutions of a lattice of period d . By non-trivial we mean solutions not immediately obvious from the fact that a solution with period d is also a solution of period $2d$. Non-trivial period-doubled solutions are caused by the nonlinearity in the mean field of the condensate [17]. They do not appear in the linear Schrödinger equation and therefore have no analog in linear band theory. Our way of understanding swallowtails is valid for both repulsive and attractive condensates, unlike previous explanations [26].

We used the two-color lattice to adiabatically connect the one-color lattice of period d and $2d$. We showed that swallowtails appear in the band structure of the two-color lattice even for weak nonlinearity, unlike in the one-color case. We then made explicit predictions for the onset of instability in the band structure for the one- and two-color lattices based on numerical simulations. Instability is experimentally observable as an increased loss rate due to heating of the condensate [31], and weak nonlinearity is the present regime of experimental investigation.

Our studies utilized a two-color Kronig-Penney potential. In order to justify the use of this model we compared analytic solutions to the one-color Kronig-Penney [21], Jacobi elliptic [18], and sinusoidal potentials [16]. We showed that each of these models resulted in a similar band structure. Moreover, by putting the exact solutions to the Jacobi elliptic potential in Bloch wave form, we were able to resolve a longstanding question concerning density offsets and stability in the work of Bronski *et al* [18, 19].

We note that there are other solution types than the ones we have considered. For instance, there are gap solitons [25, 36, 47] and time-periodic solutions [42, 48]. These can have novel features in the two-color lattice [25]. We emphasize that we have treated only the superfluid phase of cold bosons on a lattice [49, 50].

Acknowledgments

We thank Eugene Zaremba and Christopher Pethick for useful discussions. Support is acknowledged for B.T.S. and M.J.H. from the National Science Foundation and for L.D.C. from the U.S. Department of Energy, Office of Basic Energy Sciences via the Chemical Sciences, Geosciences and Biosciences Division.

[1] M. H. Anderson, J. R. Ensher, M. R. Matthews, C. E. Wieman, and E. A. Cornell, *Science* **269**, 198 (1995).

[2] K. B. Davis, M.-O. Mewes, M. R. Andrews, N. J. van Druten, D. S. Durfee, D. M. Kurn, and W. Ketterle,

- Phys. Rev. Lett. **75**, 3969 (1995).
- [3] C. C. Bradley, C. A. Sackett, J. J. Tollett, and R. G. Hulet, Phys. Rev. Lett. **75**, 1687 (1995).
- [4] B. Eiermann, T. Anker, M. Albiez, M. Taglieber, P. Treutlein, K. P. Marzlin, and M. K. Oberthaler, Phys. Rev. Lett. **92**, 230401 (2004).
- [5] T. Anker, M. Albiez, B. Eiermann, M. Taglieber, and M. K. Oberthaler, Opt. Express **12**, 11 (2004).
- [6] B. P. Anderson and M. A. Kasevich, Science **282**, 1686 (1998).
- [7] E. W. Hagley, L. Deng, M. Kozuma, J. Wen, K. Helmerston, S. L. Rolston, and W. D. Phillips, Science **283**, 1706 (1999).
- [8] Y. B. Ovchinnikov, J. H. Müller, M. R. Doery, E. J. D. Vredenbregt, K. Helmerston, S. L. Rolston, and W. D. Phillips, Phys. Rev. Lett. **83**, 284 (1999).
- [9] J. L. Roberts, N. R. Claussen, J. P. Burke, Jr., C. H. Greene, E. A. Cornell, and C. E. Wieman, Phys. Rev. Lett. **81**, 5109 (1998).
- [10] A. Inouye, M. R. Andrews, J. Stenger, H.-J. Miesner, D. M. Stamper-Kurn, and W. Ketterle, Nature (London) **392**, 151 (1998).
- [11] J. Sacher, D. Baums, P. Panknin, W. Elsasser, and E. O. Gobel, Phys. Rev. A **45**, 1893 (1992).
- [12] T. B. Simpson, J. M. Liu, A. Gavrielides, V. Kovanis, and P. M. Alsing, Appl. Phys. Lett. **64**, 3539 (1994).
- [13] B. Wu and Q. Niu, Phys. Rev. A **64**, 061603(R) (2001).
- [14] D. Diakonov, L. M. Jensen, C. J. Pethick, and H. Smith, Phys. Rev. A **66**, 013604 (2002).
- [15] B. Wu, R. B. Diener, and Q. Niu, Phys. Rev. A **65**, 025601 (2002).
- [16] M. Machholm, C. J. Pethick, and H. Smith, Phys. Rev. A **67**, 053613 (2003).
- [17] M. Machholm, A. Nicolin, C. J. Pethick, and H. Smith, Phys. Rev. A **69**, 043604 (2004).
- [18] J. C. Bronski, L. D. Carr, B. Deconinck, and J. N. Kutz, Phys. Rev. Lett. **86**, 1402 (2001).
- [19] J. C. Bronski, L. D. Carr, B. Deconinck, J. N. Kutz, and K. Promislow, Phys. Rev. E **63**, 036612 (2001).
- [20] J. C. Bronski, L. D. Carr, R. Carretero-González, B. Deconinck, J. N. Kutz, and K. Promislow, Phys. Rev. E **64**, 056615 (2001).
- [21] B. T. Seaman, L. D. Carr, and M. J. Holland, Phys. Rev. A **71**, 033622 (2005).
- [22] B. T. Seaman, L. D. Carr, and M. J. Holland, Phys. Rev. A **71**, 033609 (2005).
- [23] W. Li and A. Smerzi, Phys. Rev. E **70**, 016605 (2004).
- [24] R. Roth and K. Burnett, Phys. Rev. A **68**, 023604 (2003).
- [25] P. J. Y. Louis, E. A. Ostrovskaya, and Y. S. Kivshar, Phys. Rev. A **71**, 023612 (2005).
- [26] E. J. Mueller, Phys. Rev. A **66**, 063603 (2002).
- [27] P. Meystre and M. Sargent III, *Elements of Quantum Optics*, 3rd ed. (Springer, Berlin, 1999).
- [28] J. H. Denschlag, J. E. Simsarian, H. Haffner, C. McKenzie, A. Browaeys, D. Cho, K. Helmerson, S. L. Rolston, and W. D. Phillips, J. Phys. B **35**, 3095 (2002).
- [29] L. Fallani, F. S. Cataliotti, J. Catani, C. Fort, M. Modugno, M. Zawada, and M. Inguscio, Phys. Rev. Lett. **91**, 240405 (2003).
- [30] S. Peil, J. V. Porto, B. L. Tolra, J. M. Obrecht, B. E. King, M. Subbotin, S. L. Rolston, and W. D. Phillips, Phys. Rev. A **67**, 051603 (2003).
- [31] L. Fallani, L. De Sarlo, J. E. Lye, M. Modugno, R. Saers, C. Fort, and M. Inguscio, Phys. Rev. Lett. **93**, 140406 (2004).
- [32] L. Guidoni, C. Triche, P. Verkerk, and G. Grynberg, Phys. Rev. Lett. **79**, 3363 (1997).
- [33] A. A. Sukhorukov and Y. S. Kivshar, Phys. Rev. Lett. **87**, 083901 (2001).
- [34] K. M. Hilligsoe, M. K. Oberthaler, and K.-P. Marzlin, Phys. Rev. A **66**, 063605 (2002).
- [35] P. G. Kevrekidis, R. Carretero-Gonzalez, G. Theocharis, D. J. Frantzeskakis, and B. A. Malomed, Phys. Rev. A **68**, 035602 (2003).
- [36] P. J. Y. Louis, E. A. Ostrovskaya, C. M. Savage, and Y. S. Kivshar, Phys. Rev. A **67**, 013602 (2003).
- [37] M. Olshanii, Phys. Rev. Lett. **81**, 938 (1998).
- [38] L. D. Carr, C. W. Clark, and W. P. Reinhardt, Phys. Rev. A **62**, 063610 (2000).
- [39] L. Salasnich, A. Parola, and L. Reatto, Phys. Rev. A **65**, 043614 (2002).
- [40] E. P. Gross, Nuovo Cimento **20**, 454 (1961).
- [41] L. P. Pitaevskii, Zh. Eksp. Teor. Fiz. **40**, 646 (1961), [Sov. Phys. JETP **13**, 451 (1961)].
- [42] M. A. Porter and P. Cvitanovic, Phys. Rev. E **69**, 047201 (2004).
- [43] B. Wu and D. I. Choi, Phys. Lett. A **318**, 558 (2003).
- [44] L. D. Carr, C. W. Clark, and W. P. Reinhardt, Phys. Rev. A **62**, 063611 (2000).
- [45] *Handbook of Mathematical Functions*, edited by M. Abramowitz and I. A. Stegun (National Bureau of Standards, U.S. and GPO, Washington, D.C., 1964).
- [46] L. DeSarlo, L. Fallani, J. E. Lye, M. Modugno, R. Saers, C. Fort, and M. Inguscio, e-print cond-mat/0412279v1 (2004).
- [47] I. M. Merhasin, B. V. Gisin, R. Driben, and B. A. Malomed, Phys. Rev. E **71**, 016613 (2005).
- [48] M. A. Porter, P. G. Kevrekidis, and B. A. Malomed, Physica D **196**, 106 (2004).
- [49] M. P. A. Fisher, P. B. Weichman, G. Grinstein, and D. S. Fisher, Phys. Rev. B **40**, 546 (1989).
- [50] M. Greiner, O. Mandel, T. Esslinger, T. W. Hansch, and I. Bloch, Nature (London) **415**, 39 (2002).